A Flexible Approach to the Calculation of Resonance Energy Transfer Efficiency between Multiple Donors and Acceptors in Complex Geometries

Ben Corry,* Dylan Jayatilaka,* and Paul Rigby†
*School of Biomedical, Biomolecular and Chemical Sciences, †Biomedical Imaging and Analysis Facility, The University of Western Australia, Crawley, Australia

ABSTRACT Resonance energy transfer provides a practical way to measure distances in the range of 10–100 Å between sites in biological molecules. Although the relationship between the efficiency of energy transfer and the distance between sites is well described for a single pair of fluorophores, the situation is more difficult when more than two fluorophores are present. Using a Monte Carlo calculation scheme, we demonstrate how resonance energy transfer can be used to measure distances between fluorophores in complex geometries. We demonstrate the versatility of the approach by calculating the efficiency of energy transfer for individual fluorophores randomly distributed in two and three dimensions, for linked pairs of donors and acceptors and pentameric structures of five linked fluorophores. This approach can be used to relate the efficiency of energy transfer to the distances between fluorophores, R_0, molecular concentrations, laser power, and donor/acceptor ratios in ensembles of molecules or when many fluorophores are attached to a single molecule such as in multimeric proteins.

INTRODUCTION

Resonance energy transfer is a photochemical process whereby one fluorescent molecule or fluorophore, the ''donor'', excited by an initial photon of light (usually supplied by a laser), spontaneously transfers its energy to another molecule, the ''acceptor'', by a nonradiative dipole-dipole interaction (1–3). If the acceptor is itself fluorescent, the process is generally termed fluorescence (or Förster) resonance energy transfer (i.e., FRET).

FRET is a particularly useful tool in molecular biology as the fraction, or efficiency, of energy that is transferred can be measured (4), and depends on the distance between the two fluorophores. The distance over which energy can be transferred is dependent on the spectral characteristics of the fluorophores, but is generally in the range 10–100 Å. Thus, if fluorophores can be attached to known sites within molecules, measurement of the efficiency of energy transfer provides an ideal probe of inter- or intramolecular distances over macromolecular length scales. Indeed, fluorophores used for this purpose are often called ''probes''.

Techniques for measuring FRET are becoming more sophisticated and accurate, making them suitable for a range of applications (4). FRET has been used for measuring the structure (5–7), conformational changes (8) and interactions between molecules (9,10), and as a powerful indicator of biochemical events (11). Further applications can be found in the reviews of Van der Meer et al. (2), Lakowicz (12), or Selvin (13).

Although the challenges of labeling molecules with fluorophores and making accurate measurements of the fluorescence emitted by them are being overcome, a number of difficulties still remain when examining real-life systems. One such theoretical challenge involves linking the measured efficiency of energy transfer to the distance between the participating fluorophores. Although the relationship has been well described for a single donor-acceptor pair, it has often been stressed that a system with multiple donors and multiple acceptors cannot be described by this single distance model (12,14). Many current and potential applications of FRET involve multiple fluorophores, either because there are many target molecules within the imaged sample, or because it is impossible to have only one donor-acceptor pair within a given molecule. For example, there may be many sites on the one molecule to which donors or acceptors could bind, or many intrinsic fluorophores within the molecule of interest.

One way to avoid some of these problems is to improve the experimental apparatus such that measurements are made on single molecules (15,16). Such techniques have allowed for measurements of FRET between single donor and acceptor pairs, the dynamics of single molecules (17–19), and the examination of subpopulations of molecules (20,21).

The use of detailed theoretical analysis provides another path to relate transfer efficiency and fluorophore separations when many probes are present. This allows information to be obtained without the requirement to study single molecules. Even using single molecule techniques, it is essential to be able to calculate the expected efficiency of energy transfer between all the fluorophores present, a situation that is not simple if a single target molecule contains multiple fluorescent probes.

Analytical calculations of energy transfer between multiple donors and acceptors are complex. Even the simplest situations, that of fluorophores homogeneously and randomly

Submitted June 22, 2005, and accepted for publication September 2, 2005.

Address reprint requests to Ben Corry, Tel.: 61-8-6488-3166; Fax: 61-8-6488-1005; E-mail: ben@theochem.uwa.edu.au.

0006-3495/05/12/3822/15 $2.00

doi: 10.1529/biophysj.105.069351

distributed in one, two, or three dimensions, including the assumption that the diffusion rate of the fluorophores is much slower than the transfer rate, are difficult to describe. Förster managed to characterize the donor intensity decay and quantum yield for fluorophores in three dimensions (1) and similar expressions for the intensity decay in two dimensions are also known (22–24). The situation, however, becomes even more difficult when the probes are not distributed randomly. For example, if the probes are attached to proteins, then there are excluded volumes in which other probes cannot reside. Although analytic expressions have been derived for a couple of situations (assuming two dimensions and circular excluded regions of radii much less or much greater than the distance of energy transfer) (25,26), such situations are much more amenable to numeric approaches.

Numerical Monte Carlo schemes have been used to calculate FRET between fluorophores constrained in many geometries. Snyder and Frieri (27), for example, examined the quenching of donor fluorescence obtained with fluorophores distributed in two dimensions. Zimet et al. (28) examined FRET between donors linked to membrane proteins and acceptors in lipid membranes, and estimated transfer efficiencies by calculating the quantum yield decrease for one donor in the presence of multiple acceptors. Demidov (29), on the other hand, calculated energy transfer efficiency using the mean of randomly generated decay rates. More recently, a simpler Monte Carlo technique has been developed in which FRET events are simulated explicitly (14,30). Frederix et al. (30) used this scheme to calculate FRET taking place between fluorophores on actin filaments including the possibility of photobleaching. More recently, Berney and Danuser (14) extended this scheme to examine transfer between probes distributed on a surface. They also introduced a competitive approach in which already excited acceptors could not participate in further energy transfer, and calculated transfer efficiencies directly from the fraction of absorbed photons that are transferred to acceptors.

In this article, we extend the Monte Carlo calculation scheme to a number of new cases, making it useful for a variety of practical situations. We show how this approach is suitable to calculate FRET between fluorophores distributed in any geometry. In particular, we examine fluorophores distributed randomly in two or three dimensions, and then apply the technique to more complex situations. We examine ensembles of linked donor-acceptor pairs in three dimensions with excluded volumes and then consider the case of five fluorophores attached to a single molecule as might arise when examining proteins with fivefold symmetry, such as ligand-gated ion channels (31). The approach is demonstrated for a single molecule and an ensemble of such molecules and compared with analytic results for the single molecule case. The Monte Carlo scheme developed here provides a powerful tool for calculating the efficiency of energy transfer between multiple fluorophores, either in ensembles or attached to single molecules. A simple computer program has been written to make this tool easily accessible.

METHODS

Theory for a single fluorophore pair

The theory of resonance energy transfer in a donor-acceptor pair has long been understood. Excellent descriptions can by found in a number of reviews (2,3,12) and so only a summary is given here so the notation used later can be understood. As shown by Förster (1,32) the rate of energy transfer from one fluorophore to another is dependent on the inverse sixth power of the distance between them, r, due to the dipole-dipole nature of the electronic excitation involved. Indeed, the rate can be simply expressed as

$$k_T(r) = \frac{1}{\tau_D}\left(\frac{R_0}{r}\right)^6, \tag{1}$$

in which R_0 is termed the characteristic or *Förster* distance at which the rate of energy transfer is equal to the decay rate of the donor fluorophore, and τ_D is the decay rate of the donor in the absence of an acceptor. This characteristic distance is dependent on the spectral characteristics of the fluorophores, in particular the quantum yield of the donor, the spectral overlap of the donors emission and acceptors absorption spectra, the extinction coefficient of the acceptor, the refractive index of the medium, and the relative orientation of the donor and acceptor dipoles.

More commonly, energy transfer is described by its efficiency, E, the fraction of photons absorbed by the donor that are transferred to the acceptor. Expressing this in terms of rates yields

$$E = \frac{k_T}{\tau_D^{-1} + k_T} \tag{2}$$

$$= \frac{1}{1 + \left(\frac{r}{R_0}\right)^6}. \tag{3}$$

The characteristic distance, R_0, can now be interpreted as the distance at which half the energy absorbed by the donor is transferred to the acceptor.

Monte Carlo calculation scheme

The efficiency of energy transfer is calculated in this article using a Monte Carlo scheme similar to that developed by Berney and Danuser (14). The idea for the scheme is straightforward. The efficiency of energy transfer for a given configuration of fluorophores is calculated by modeling the incoming radiation by a discrete series of photons. These incoming photons or ''excitons'' cause the excitation of the donors for a period of time during which they cannot absorb another photon, but may become de-excited again either through the emission of a photon (fluorescence) or else transfer energy to an acceptor, which then remains excited for a period of time during which it is not available for further energy transfer. The term *exciton* is used rather than *photon* to account for the fact that only photons that strike a donor and could possibly be absorbed are considered. A count is maintained of the number of energy transfer events and the number of fluorescence events from which the efficiency of energy transfer is easily calculated. The steps involved in this calculation are illustrated schematically in Fig. 1 and are described in detail below. The case of donor florescence being reabsorbed by another fluorophore has not been considered, as the probability of this occurring is much smaller than the probability of absorption from the illuminating laser; however, this could be included in a development of the algorithm.

Step 1—Assign fluorophore positions and types

The first step is to generate realistic ensembles of fluorophores coordinates, the configurations from which the FRET efficiencies can be calculated.

One of the main contributions of this article has been the development of a method for assigning fluorophore coordinates for a number of common

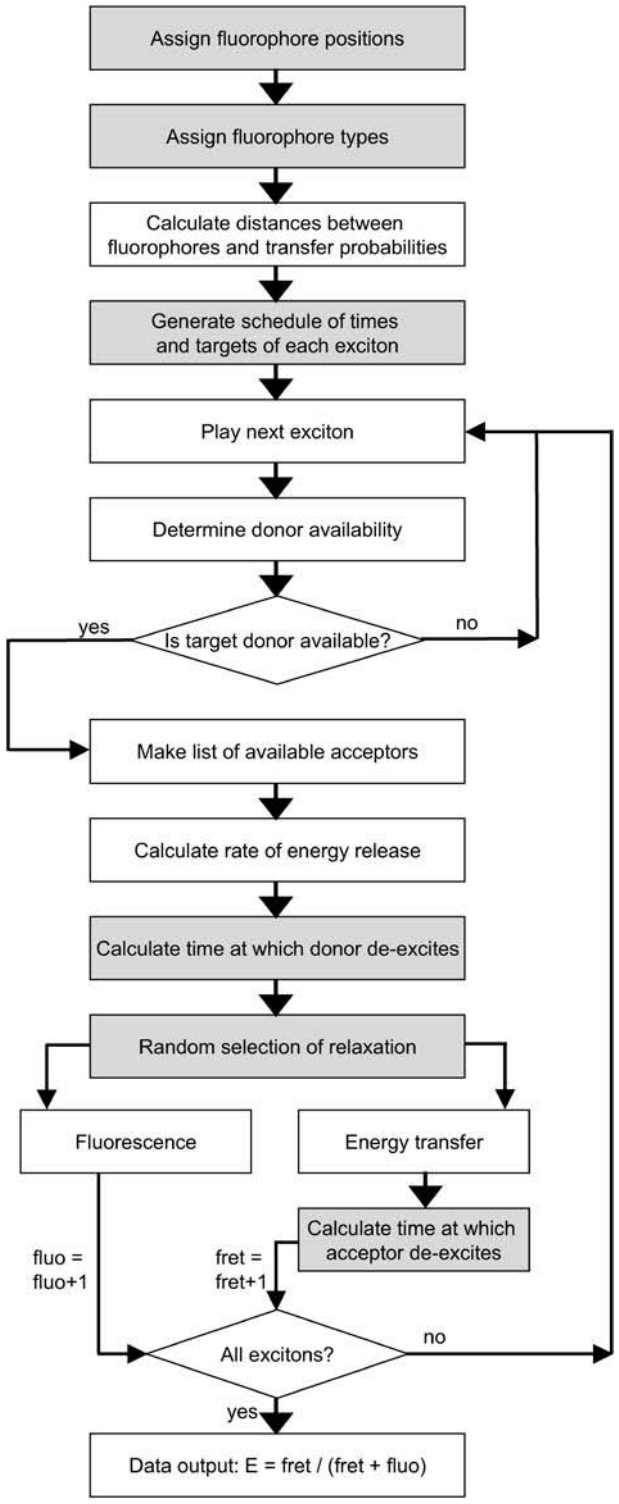

FIGURE 1 Flowchart of the steps involved in the Monte Carlo calculation scheme. Processes involving a random number generator are indicated by a shaded background. Figure adapted from similar figures by Frederix et al. (30) and Berney and Danuser (14).

situations in which the fluorophores are distributed in either two or three dimensions. This coordinate assignment method takes into account the fact that the fluorophores are usually attached to a host molecule at specific points on the molecular framework. It also accounts for the fact that the host molecules occupy a finite region of space. Such constraints are found when, for example, the fluorophores are attached to proteins which are randomly distributed in a two-dimensional membrane, or in a three-dimensional cell volume.

Step 1.1—Accounting for the regular arrangement of the fluorophores. Fluorophores are assumed to be part of n-mer structures, in which n fluorophores are linked in a fixed orientation with respect to each other. For $n = 1$, individual fluorophores are distributed randomly. For $n = 2$, they are linked in pairs with a specified separation. For $n \geq 3$, n fluorophores are distributed on the radius of either a circle (in the case of two or three dimensions) or surface of a sphere (in the case of three dimensions). These latter fluorophore groups are the general n-mers on which the FRET simulation is based. The center of the circle or sphere is the position of the n-mer. In the following, we refer only to the three-dimensional case; the two-dimensional case is the same, except that any sphere must be replaced by a circle.

Step 1.2—Accounting for excluded volume effects efficiently. The n-mers are initially assigned random positions within a sphere. This sphere represents the volume of the sample in which the n-mers are able to move. In our case, we ensure that none of the n-mers overlap: there is an excluded volume around the center of each n-mer (represented by another sphere) in which no other fluorophores can reside. This simulates the fact that the fluorophores are attached to a host molecule that occupies the excluded spherical region, and this host molecule prevents others from occupying the same space. More elaborate excluded volume schemes that depend on the shape and orientation of the host molecule may be imagined, but such schemes do not change the basic recipe described here.

When the size of the host molecules and their concentration is large, it can be difficult to find allowed coordinates for the n-mers as many molecules have to be packed into a confined space. To overcome this problem, the coordinates are assigned using an annealing procedure. In this, molecules are initially assigned random coordinates. If overlaps exist, then new coordinates are again randomly assigned for one of the overlapping molecules. The new configuration is kept if it reduces the number of overlaps, or if a random number generated between 0 and 1 is less than an annealing parameter. The procedure is repeated, slowly reducing the annealing parameter until no overlaps exist. By using the annealing parameter, new coordinates that do not reduce the number of overlaps are occasionally used to avoid situations where accepting only nonoverlapping coordinates is not possible. In our case, we initially set the annealing parameter to 0.3, and it is slowly reduced to zero over 35,000 steps. When the concentration of n-mers is too large, it becomes impossible to obtain nonoverlapping coordinates.

If the fluorophores are not associated in n-mers (i.e., $n = 1$), then assigning coordinates is straightforward, since excluded volumes do not have to be taken into account. In this case, the fluorophores are given random positions. In all other cases, once the n-mers have been assigned coordinates, the fluorophores are distributed symmetrically around the surface of the n-mer with random orientations.

Step 1.3—Assign fluorophore type. Once the locations of each fluorophore have been assigned, the fluorophores are then randomly assigned to be either donors or acceptors, assuming certain values for the probability of each location being either a donor or acceptor. This simulates the fact that the fluorophores are attached to the host molecule by mixing a solution containing a fixed ratio of the fluorophores with the prepared host molecule, under conditions such that the likelihood of one fluorophore attaching to the prepared host molecule is independent of whether another fluorophore has already attached.

For most of the calculations below, the probability of any fluorophore being a donor is taken to be equal to that of being an acceptor. However, in some cases we adjust this probability to set the donor/acceptor ratio. Also, in the case of fluorophore pairs ($n = 2$) discussed below, we make sure that there is always one donor and one acceptor in each pair, as if the separate host molecules had been specifically labeled this way. If the donor and acceptor fluorophores were binding to different sites on the host molecule for $n > 2$, rather than competing for the same locations as described here, then the assignment of fluorophore types and coordinates could easily be extended to make sure the appropriate geometry of donor and acceptor molecules was accurately reproduced.

Step 2—Calculate transfer probability factors

Once the positions and type of each fluorophore has been assigned, the transfer probability P_{ij} from each donor i to every acceptor j is calculated from the expression

$$P_{ij} = \frac{R_0^6}{r_{ij}^6}, \tag{4}$$

where r_{ij} is the distance between them and R_0 is the Förster distance specific to each fluorophore pair, at which the rate of energy transfer is equal to the decay rate of the donor fluorophore. This probability is stored in a matrix for use below. The value of the Förster distance, R_0, is dependent (among other things) on the spectral overlap of the fluorophores as well as the relative orientation of their transition dipoles. In our procedure, we specify the value of this parameter R_0 explicitly in the input file. Thus we do not assume any particular orientations or orientation factor (known as κ^2), but rather leave this to be included in the value of R_0 specified by the user.

Step 3—Calculate exciton flux

The rate at which excitons strike the system is dependent on the properties of the illuminating laser and the size of the simulated area. Rather than specify the exciton flux directly in the input to the Monte Carlo program as has been done previously (14), we specify the properties of the laser and fluorophores and calculate the flux of excitons incident on the simulation system from these. The flux of photons incident on the simulation system will be given by

$$f_p = \frac{\pi r^2 I \lambda}{hc}, \tag{5}$$

where r is the radius of the simulated system, I is the irradiance of the illuminating laser, λ is the wavelength of the laser, h is Planck's constant, and c is the speed of light. Only some of these photons will be absorbed by the fluorophores, thus the flux of excitons will be given by $f_e = f_p{*}A$, where A is the absorbed fraction which can be determined from the equation

$$A = 1 - 10^{-\epsilon c L}, \tag{6}$$

in which ϵ is the extinction coefficient of the donor fluorophores, c is their concentration, and L is the pathlength of the laser through the simulation system. For circular or spherical systems with homogeneous distributions of n-mers, it can be shown that

$$f_e = \frac{\pi r^2 I \lambda}{hc}\left[1 - 10^{\frac{-\varepsilon n_d}{1000 N_A \pi r^2}}\right], \tag{7}$$

where n_d is the number of donor fluorophores in the simulation.

Step 4—Generate exciton schedule

Based on the flux of incident excitons, the time interval over which excitons are incident on the fluorophores is calculated. The excitons are then randomly assigned an incidence time within this interval, a target donor, and arranged in chronological order.

Step 5—Play excitons

The excitons are then played to see if they are absorbed by the donor, and if so, whether and where energy is transferred, as described in the following steps.

Step 5.1—Check fluorophore availability. Initially all the donors are unexcited and available to absorb incident excitons. However, after the first exciton has been played it is possible that one or more donors are already excited, and so these donors cannot absorb another exciton. Likewise, after the first energy transfer event, some of the acceptors may already be in an excited state where they are unable to accept further energy. Therefore, two lists must be maintained: one for donors that are unavailable to accept an exciton, and a corresponding unavailable list for the acceptors.

The unavailable list for the donors is made by assuming that the k^{th} target donor becomes excited at the time T_k of the incoming exciton, and it remains excited for a period T_d (calculated below; see Eq. 8) until $T_k + T_d$. Likewise, if an acceptor becomes excited (see Step 5.2), then it remains excited for a period T_a (see Eq. 11) until $T_k + T_a$. Although an acceptor molecule involved in energy transfer will, in reality, only become excited during the interval after the donor de-excites, $T_k + T_d$ to $T_k + T_d + T_a$, here we have assumed the acceptor is unavailable during the interval $T_k + T_a$. This avoids computational difficulties of priority when two donors attempt to transfer energy to the same acceptor and will not influence the final results. Knowing the period for which the acceptors and donors are excited, the unavailable lists may be constructed and updated at the time any exciton is played.

If the target donor for the current exciton is on the unavailable list, then the exciton is lost, and we move on to the next exciton in the chronological sequence. Otherwise, the donor accepts the exciton, is placed on the unavailable list, and the time at which the donor releases its energy is recorded.

The time taken for the donor to release its energy in the simulation is calculated as (14)

$$T_d = -\tau_T \ln \gamma_d, \tag{8}$$

where γ_d is a uniformly distributed random number in the range 0–1, and where τ_T is the energy release rate for the donor (14,29),

$$\tau_T^{-1} = \tau_D^{-1}\left(1 + \sum_{j=1}^{a_{free}} P_{ij}\right). \tag{9}$$

Here, τ_D is the lifetime of the unquenched donor, available from experimental measurements, and a_{free} is the number of available acceptors which are not excited at the time that the donor absorbs its energy.

Once a fluorophore releases its energy it once more becomes available to absorb later excitons.

Step 5.2—Determine if donor fluoresces or transfers energy. The excited donor can either release its energy by fluorescing, or by transferring its energy. The probability of either fluorescence, or transfer to acceptor j is given by

$$\frac{\tau_T}{\tau_D}, \quad \text{or} \quad \frac{\tau_T}{\tau_D} P_{ij}, \tag{10}$$

respectively. The mode of de-excitation is thus determined in a probabilistic fashion by creating a cumulative histogram of each of the possible energy release pathway (fluorescence, energy transfer to acceptor 1, energy transfer to acceptor 2...), picking a uniform random number in the range 0–1 and seeing within which release class it falls.

If the donor fluoresces, then a variable *fluo* is incremented by 1. If the donor transfers energy to an acceptor, then a variable *fret* is incremented by 1. These variables are used to calculate the energy transfer efficiency relative to fluorescence.

If the donor transfers energy, then the time interval for which the acceptor is unavailable is calculated using

$$T_a = -\tau_A \ln \gamma_a, \tag{11}$$

in which τ_A is the acceptor lifetime and γ_a is another random number in the range 0–1.

Although all donors and acceptors in the system can absorb incident excitons or transferred energy, to avoid boundary effects caused by having a finite-sized system (apart from in the single-molecule case described later), we do not include energy released from donors within a buffer region near the boundaries of the system in our calculation of FRET efficiency. We set the width of this region to be two-times the Förster distance as described below.

Step 5.3—Repeat for all excitons. The above Steps 5.1 and 5.2 are repeated for all the excitons.

Step 6—Calculate FRET efficiency

Finally the FRET efficiency, E, can be calculated by comparing the number of donors that fluoresce and the number that undergo energy transfer:

$$E = \frac{fret}{fret + fluo}. \tag{12}$$

Step 7—Repeat FRET calculation for many configurations

The entire process, Steps 1–6, is repeated for many randomly created fluorophore configurations. The FRET efficiency for all the configurations is then averaged and output.

It should be noted that this strategy for computing the efficiency of energy transfer (Steps 4–6) is the same as that used by Berney and Danuser (14). The main difference from their work has been to apply this technique to different geometrical distributions of fluorophores, which are particularly relevant for elucidating the geometrical structure of proteins and to provide a general interface for carrying out the calculations.

In Fig. 2, we indicate how the results of the simulation described in more detail below depend upon the choice of simulation parameters for the case of fluorophores randomly distributed in three dimensions. Increasing the number of fluorophores in the simulation, the number of configurations, or the number of excitons acts to improve the averaging procedure and thus yields a more accurate result for the average transfer efficiency expected in a large sample. However, it can be seen that, provided each of these values is larger than a couple of hundred, the final result is barely affected and the efficiency values are accurate to two decimal places. The size of the buffer region is more important. Fluorophores near the edge of the simulation have fewer neighbors, and so the chance of them transferring energy is lower. Thus, when no buffer region is used, the efficiency values are underestimated. As shown in Fig. 2 *B*, the efficiency values quickly converge to a stable value as the buffer size is increased. For the remainder of the results, we use a buffer size of $2R_0$.

The Monte Carlo calculation scheme was enacted in FORTRAN90. The meanings and units of the parameters used in this study are indicated in Table 1. Further details of the computer program are given in Appendix B.

The time taken to calculate the efficiency varies considerably depending on the situation. In general, a curve containing 20 points for the efficiency of energy transfer versus the concentration of randomly distributed fluorophores can be calculated to a high degree of accuracy within 15 min on a Pentium 2.4-GHz PC. Generating configurations is slowest in the cases of excluded volumes (i.e., many pentamers or donor-acceptor pairs) when both the *n*-mer size and density are large, since it becomes harder to fit these volumes into the confined space. The time taken to complete a calculation is therefore highly dependent on the size of the molecules, and the curves plotted here take from 10 to 60 min to compute.

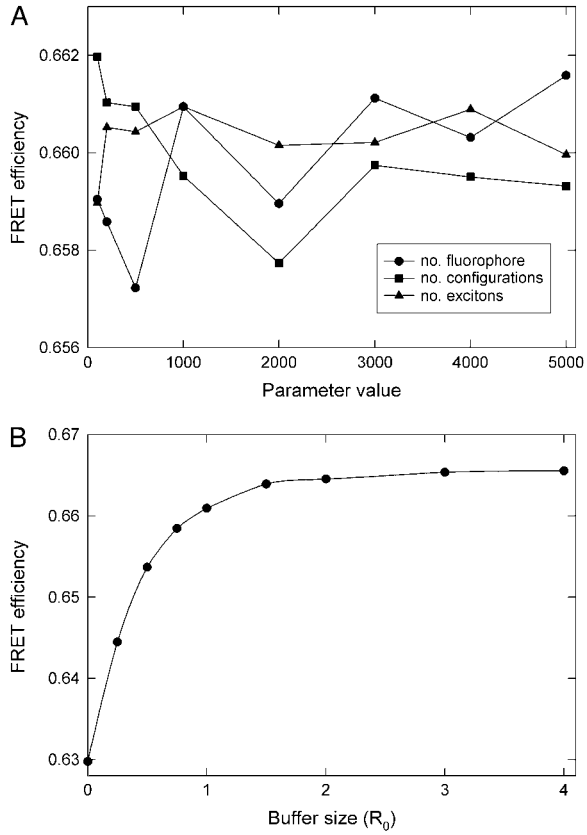

FIGURE 2 Influence of parameter values on transfer efficiency in Monte Carlo efficiency calculations. (*A*) The transfer efficiency is plotted while changing the number of fluorophores (*circles*), number of configurations (*squares*), and number of excitons (*triangles*). When one parameter is altered, the value of the other two is set to 1000. (*B*) The transfer efficiency is plotted versus the buffer size (shown in units of R_0). Calculations are made for fluorophores randomly distributed in three dimensions at a concentration of 3 mM, $R_0 = 60$ Å, and an irradiance of 1×10^{-15}.

RESULTS

Randomly distributed fluorophores in three dimensions

If donor and acceptor fluorophores are dissolved in solution, energy transfer can be expected to take place whenever the fluorophores come close to one another. Indeed, the average efficiency of energy transfer will depend on their average separation, and thus the concentration of fluorophores. In Fig. 3 we plot the result of a Monte Carlo calculation relating the efficiency of energy transfer to the concentration of fluorophores in solution. It can be seen that the efficiency

TABLE 1 Values and meanings of parameters

Parameter	Value	Meaning
R_0	20–60 Å	Characteristic distance for fluorophore pair.
I	0–10 W/μm^2	Irradiance of illuminating laser (default 1×10^{-15}).
λ	488 nm	Wavelength of illuminating laser.
ϵ	70,000 cm^{-1} M^{-1}	Donor extinction coefficient.
τ_D	1 ns	Donor fluorescence lifetime in the absence of acceptors.
τ_A	1 ns	Acceptor fluorescence lifetime.
n	1000–2000	Number of fluorophores used per calculation.
n_c	1000–5000	Number of configurations used per calculation.
n_e	1000–5000	Number of excitons used per configuration.
P_d	0.1–0.9	Probability of any fluorophore being a donor (default 0.5).
	2.0	Buffer size.

increases rapidly as the concentration of increases. At high concentrations, the efficiency of energy transfer approaches *1*, as many acceptor molecules are likely to reside within the characteristic distance of the donor. The transfer efficiency is also strongly dependent on R_0. Measurements of efficiency in solution are simple to carry out and thus provide a good experimental test of calculated R_0 values for fluorophore pairs.

It is apparent, however, that the number and proportion of available (i.e., not already excited) acceptor molecules around each donor will influence the transfer rate. One way in which this can be altered is by changing the rate at which photons strike the sample. When the exciting laser is set to a very low intensity, such that the average rate of excitation τ_E^{-1} for each donor is much less than the average decay rate of both the donors and acceptors τ_T^{-1}, then both

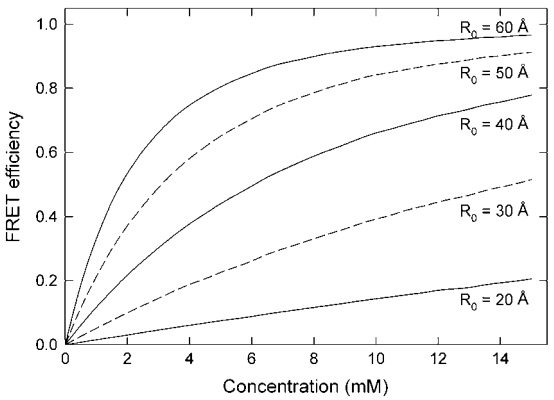

FIGURE 3 FRET efficiency for fluorophores randomly distributed in solution. The FRET efficiency is plotted against the concentration of fluorophores for a number of characteristic radii R_0. The laser irradiance assumed to be small. The total concentration of fluorophores (donor + acceptor) is plotted on the x axis, with the probability of any fluorophore being a donor set to 0.5.

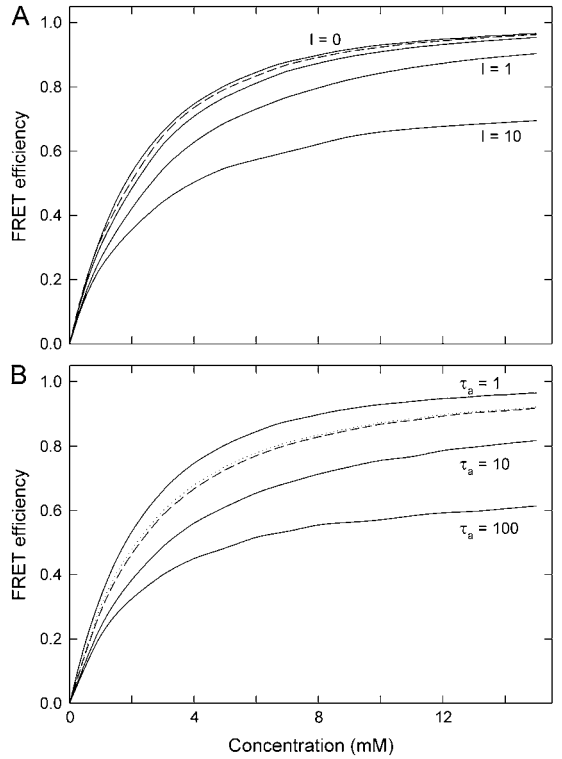

FIGURE 4 The influence of irradiance and fluorophore lifetime on the transfer efficiency. (*A*) The transfer efficiency is plotted versus the total concentration of fluorophores randomly distributed in three dimensions for a variety of laser irradiance values. Irradiance values of 0, 0.01, 0.1, 1.0, and 10 W/μm^2 are used as indicated. (*B*) The transfer efficiency is plotted against the acceptor lifetime (indicated in nanoseconds) assuming a donor lifetime of 1 ns and an irradiance of 0.1 W/μm^2. Also shown is the effect of increasing the donor lifetime to 100 ns while holding the acceptor lifetime at 1 ns (*dotted line*) and the result with an irradiance of 0.01 W/μm^2 and an acceptor lifetime of 10 ns (*dashed line*). A characteristic distance of $R_0 = 60$ Å is used throughout with the donor/acceptor ratio set to 1.

will have decayed before the next photon appears. On the other hand, if the incident flux is high, fluorophores will often be unavailable to participate in energy transfer, and so many photons will not be absorbed, and more donors will fluoresce rather than transferring energy.

In Fig. 4 *A*, we plot how the efficiency of energy transfer depends on the irradiance of the exciting laser. With a low irradiance, the transfer efficiency approaches *1* at high concentration. At high irradiance the efficiency rises more slowly.

Given that the laser irradiance can affect the overall efficiency of energy transfer, it is worth considering how the values discussed here compare to those that would exist in a typical experimental setup. Following the calculations of Pawley (33), a laser with power 1 mW, wavelength 633 nm, an objective of NA = 1.4, refractive index 1.52, and 60% transmission through the lens, yields an irradiance of 0.01 W/μm^2 at the sample. The authors typically use a 488-nm Argon laser with a 3% transmission neutral density filter, which produces 100 μW of power before entering the

objective. Assuming a 60% transmission though the water immersion objective lens (33), this has an irradiance of only 0.001 W/μm^2. Even without a transmission filter, this laser has a maximum irradiance of only ~0.02 W/μm^2. Comparing these values to those plotted in Fig. 4 *A*, it appears unlikely that the laser power will significantly alter the transfer efficiency measured in this case; however, caution should be applied.

Another way for the transfer efficiency to decrease is if the lifetime of the acceptor in the excited state is much longer than that of the donor fluorophores. In this case, it becomes more likely for acceptor molecules to be unavailable for transfer when a donor gets excited. In Fig. 4 *B*, we show how the transfer efficiency alters as the acceptor lifetime is increased, while the donor lifetime is held at 1.0 ns for an irradiance of 0.1 W/μm^2. It is apparent that once the acceptor lifetime is large, the transfer efficiency drops. Increasing the donor lifetime (Fig. 4 *B*, *dotted lines*), on the other hand, has a similar effect to increasing the irradiance.

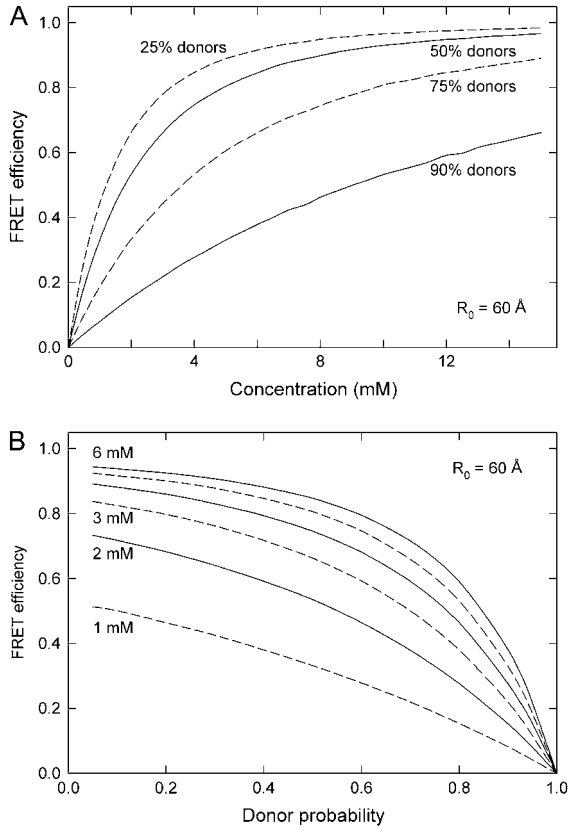

FIGURE 5 Influence of donor/acceptor ratio on the FRET efficiency for fluorophores randomly distributed in solution. (*A*) FRET efficiency is plotted against fluorophore concentration for a number of different donor/acceptor ratios. The total concentration of fluorophores (donor + acceptor) is plotted on the *x* axis. (*B*) The transfer efficiency is plotted as the proportion of donors is altered at a range of total fluorophore concentrations (1–6 mM). A characteristic distance of 60 Å and small irradiance is used throughout.

The chance of energy transfer taking place is also greatest when there are many acceptor fluorophores for each donor. In Fig. 5 *A* we show the efficiency of energy transfer as the ratio of donors to acceptors is altered. This is plotted more explicitly in Fig. 5 *B* where the efficiency is plotted as the proportion of fluorophores that are donors is altered at several total fluorophore concentrations. It can be seen that when there are more acceptors than donors (i.e., the probability of any given fluorophore being a donor is low), the efficiency is relatively flat. But as the proportion of donors increases above 50%, the efficiency drops rapidly toward zero. Indeed, this result could be used to determine the concentration and proportions of fluorescent solutes.

These results cannot be directly compared to analytic expressions since we found it impossible to calculate the quantities discussed here in this way. Analytic expressions usually calculate the donor intensity decay rather than the transfer efficiency (2). However, the analytic treatment introduces a critical concentration, c_0, at which the efficiency of transfer is 76% and given by

$$c_0 = \frac{3000}{2\sqrt{\pi^3} N_A R_0^3}. \quad (13)$$

This concentration agrees well with our numeric results.

Comparison with experimental results

To verify that our model correctly describes the relationship between FRET efficiency and experimental parameters, we have carried out a number of experiments involving fluorophores randomly distributed in three dimensions. In Fig. 6, we plot the results of these experiments in which AlexaFluor488 (AF488) and AlexaFluor568 (AF568) (Invitrogen-Molecular Probes, Eugene, OR) were dissolved in aqueous solution. When AF488 is excited with the 488-nm line of an argon laser, it acts as a donor transferring its energy to AF568. Assuming an orientation factor of $\kappa^2 = 2/3$ (which is likely to be appropriate when the fluorophores are freely diffusing and rotating in 3 dimensions), the spectral overlap yields a characteristic distance of $R_0 = 62$ Å. Alternatively, if we excite the mixture with the 543-nm line of a helium neon laser, this is predominantly absorbed by AF568 and it can act as a donor transferring energy to AF488. In this case, the spectral overlap is much smaller, and so $R_0 = 29$ Å. The FRET efficiency is determined by measuring the intensity in the donor emission band by the sample for both the AF488-AF568 mix (I_{da}) and a donor-only sample with the same donor concentration as the mixed sample (I_d). To do this, AF488 emission was detected through a 522/35nm bandpass filter, while AF568 emission was detected through a 585-nm long-pass filter. The efficiency is then

$$E = 1 - I_{da}/I_d, \quad (14)$$

provided the black levels and spectral bleedthrough are taken into consideration.

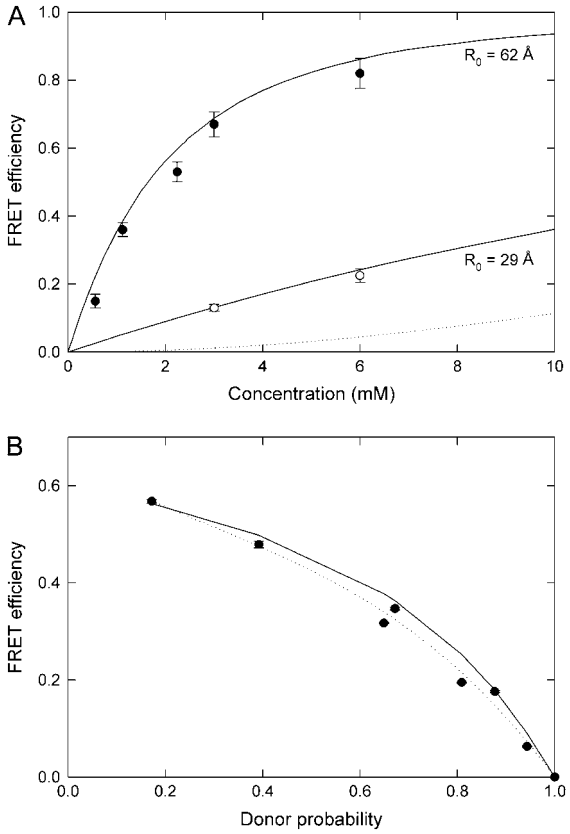

FIGURE 6 Comparison of experimental and simulated results. The FRET efficiency measured for transfer taking place between AlexaFluor488 and AlexaFluor568 dissolved in aqueous solution (*data points*) is compared to the results predicted by the Monte Carlo calculation scheme for the same conditions (*solid lines*). (*A*) The transfer efficiency is measured at a variety of total fluorophore concentrations using AF488 as the donor ($R_0 = 62$ Å) and using AF568 as the donor ($R_0 = 29$ Å). The result of the single distance model assuming $R_0 = 62$ Å is shown by the dotted line. (*B*) The FRET efficiency is calculated as the donor/acceptor ratio is varied with a total concentration between 1.2 and 2 mM. The line of best fit to the experimental data is shown by the dotted line.

In Fig. 6 *A*, we show how the FRET efficiency varies with total fluorophore (donor + acceptor) concentration with equal concentrations of donor and acceptor when exciting both AF488 (*solid circles*) and AF568 (*open circles*). Our results for both R_0 values agree well with the predictions from the Monte Carlo simulation scheme. A difficulty encountered in the experiment was to accurately determine the concentrations of the samples, because only limited quantities were being used. This introduced some uncertainty into the *x*-value of the data points. Ideally, the concentrations should be cross-checked using absorbance spectroscopy and utilizing the known extinction coefficients of the probes.

In Fig. 6 *B*, we show how the transfer efficiency depends on the donor/acceptor ratio when AF488 is used as the donor and AF568 as the acceptor. As predicted from the Monte Carlo simulation program (*solid line*), the FRET efficiency increases significantly as the proportion of acceptors to donors is increased.

TABLE 2 A comparison of measured (E_m) and predicted (E_p) transfer efficiencies for a variety of laser powers

Filter	Power (μW)	Irradiance (mW/μm^2)	E_m	E_p
0.3%	0.5	0.1	0.86 ± 0.01	0.86
1.0%	1.6	0.3	0.85 ± 0.01	0.86
3.0%	5.5	1.0	0.85 ± 0.01	0.86
10.0%	16	3.0	0.85 ± 0.02	0.86
30.0%	56	10.0	0.78 ± 0.01	0.85

Finally, we also show the effect of increasing the laser power on the FRET efficiency in Table 2. Here we excited AF488 with the 488-nm laser at a high concentration (3 mM), while varying the irradiance reaching the sample by passing the light through a variety of transmission filters. Provided the laser irradiance is low, we find very little change in transfer efficiency when the power is altered, as expected from the simulations. However, at the highest power tested, the transfer efficiency was significantly reduced—more so than the simulation predicted. This decrease in transfer efficiency is likely to be the result of photobleaching of the fluorophores that is currently not taken into consideration in the Monte Carlo simulation scheme. Thus, the use of high laser powers is likely to have a greater effect on the transfer efficiency than shown in Fig. 4.

Although the situation of fluorophores dissolved in solution appears to be a simple case in which to test our model, it contains most of the complexities of the later situations. Primarily, for any given configuration, there are many donor-acceptor separations and many possible pathways along which FRET can take place, all of which must be accurately described. Furthermore, this situation clearly cannot be characterized by a single distance model. For example, in Fig. 6 *A*, we show the results of a calculation in which the average donor to nearest acceptor separation is determined at each concentration. This is then used to calculate the transfer efficiency at each concentration using Förster's equation for transfer between a single donor and acceptor assuming $R_0 = 62$ Å. It is clear that this single distance model vastly underestimates the transfer efficiency. No doubt this is because transfer arising between neighbors that are closer than average (that is, neglected by the single distance model) can dominate the total transfer efficiency.

Randomly distributed fluorophores in two dimensions

One common use of FRET is to measure distances between fluorophores confined within a plane; for example, when they are confined within a lipid membrane or attached to a surface. Such techniques were used by Berney and Danuser (14), who distributed fluorophores in two dimensions on a monolayer of poly-(L)-lysine-*graft*-poly-ethylene-glycol to

conduct controlled tests of their FRET calculation and determination methods.

An analytic expression for rates of intensity decay (22,24) and the efficiency of energy transfer (25) has previously been calculated for this situation with the assumption that the fluorophores are always available for excitation. Numerical Monte Carlo techniques have also been applied to this situation (14,27); however, we present our numeric solutions here for completeness.

If the fluorophores can move independently within the plane, then this case is similar to the situation of fluorophores dispersed in solution. The transfer efficiency is shown in Fig. 7 and the results are similar to the case described previously. The average transfer efficiency increases as the fluorophore density increases, or equivalently as the mean separation decreases. These results are similar to those seen in a previous theoretical and experimental study (23).

Pairs of fluorophores in three dimensions

One of the most common uses of FRET is to measure the distance between a donor and acceptor fluorophore attached to a single host biomolecule. Typically the host molecules are dissolved in solution or, alternatively, are confined to a membrane plane. If the density of molecules is low, then the well-known theory of transfer between a donor and acceptor pair, Eq. 3, can be applied. However, these results can become spurious if transfer is possible between fluorophores attached to different host molecules, as might happen when their concentration is large. The Monte Carlo scheme provides an ideal way to take this possibility into account.

In Fig. 8 *A*, the FRET efficiency is plotted against the fluorophore separation for a variety of concentrations of host molecule, assuming that they are free to move in three dimensions. At low concentrations, the familiar $1/r^6$ behavior is reproduced. However, at slightly higher concentrations, the chance of energy transfer taking place between fluorophores attached to different molecules increases, and so the overall efficiency also increases. This effect is most pronounced when the fluorophore separation is large, because transfer between fluorophores attached to different host molecules becomes more likely than between fluorophores on the same host.

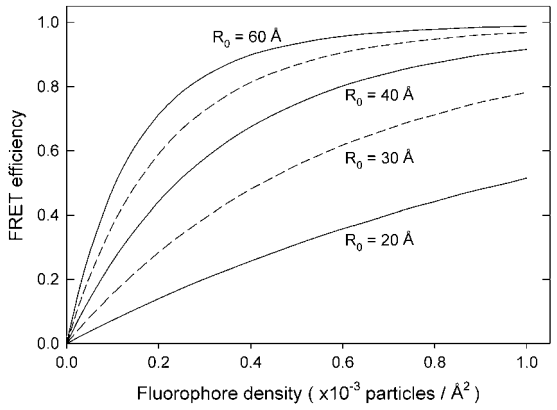

FIGURE 7 FRET efficiency for fluorophores randomly distributed in two dimensions. FRET efficiency is plotted against the total density of fluorophores (donor + acceptor) for a range of characteristic distances assuming a low irradiance and a donor/acceptor ratio of 1.

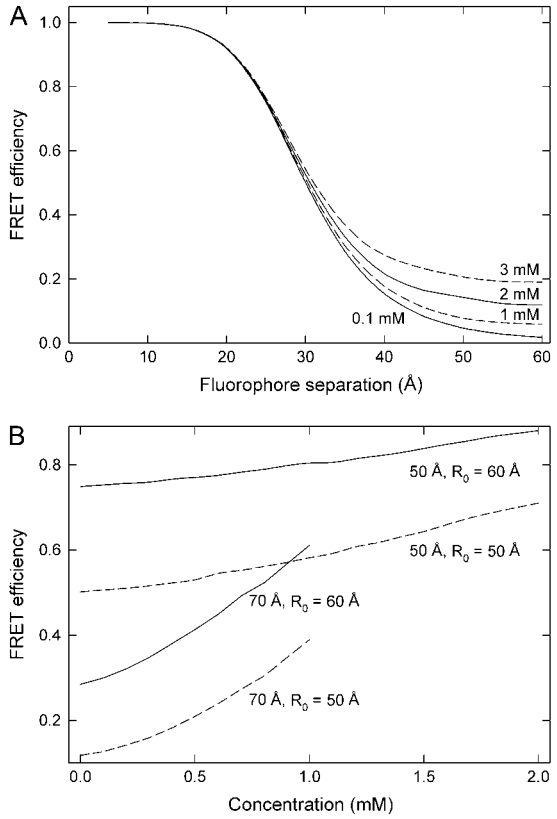

FIGURE 8 FRET efficiency for linked donor-acceptor pairs distributed in three dimensions. (*A*) FRET efficiency is plotted against the donor-acceptor separation in the pairs with $R_0 = 30$ Å. The different lines represent different concentrations of pairs. (*B*) Effect of pair concentration on transfer efficiency, plotted at two values of the donor-acceptor separation (50 Å and 70 Å) and two values of R_0 (50 Å and 60 Å) as noted on the figure.

The effect of concentration can be seen more clearly in Fig. 8 *B*, where the FRET efficiency is plotted for a pair of fluorophores separated by 50 or 70 Å at a variety of concentrations with $R_0 = 50$ or 60 Å. It is clear that the host molecule concentration can affect the average transfer efficiency, with a 1-mM change in concentration producing up to an efficiency change of >0.3. It is difficult to determine a specific concentration at which FRET between fluorophores on different hosts (intermolecular FRET) becomes important, as this will depend on the fluorophore separation on the host molecule and on the value of R_0. However, by looking at Fig. 8, it is clear that the effect can be significant in the situations studied at concentrations as low as 0.1 mM. Thus, this must be taken into account whenever relating FRET efficiency to fluorophore separation.

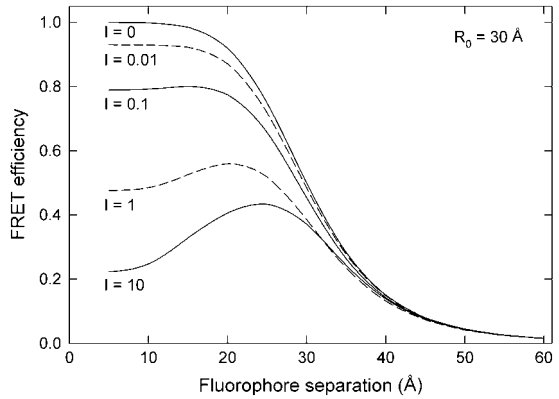

FIGURE 9 Influence of laser irradiance on transfer efficiency for linked donor-acceptor pairs. The FRET efficiency is plotted against the donor-acceptor separation in the pairs for a number of different irradiance (in units of W/μm^2) assuming a low concentration of pairs and $R_0 = 30$ Å.

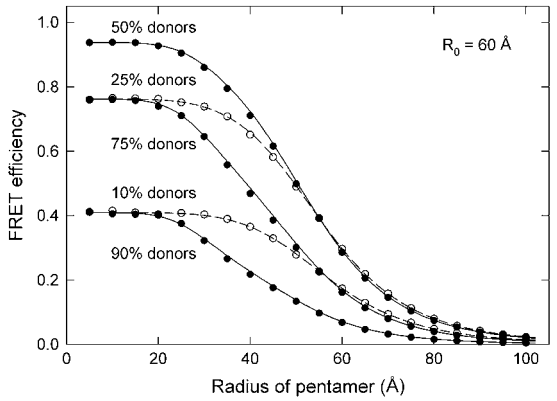

FIGURE 10 Efficiency of energy transfer between fluorophores arranged in a pentamer. The efficiency is plotted against the radius of the pentamer assuming a characteristic distance of 60 Å, while varying the donor/acceptor ratio. Analytic solutions are shown by the lines and Monte Carlo calculation by the data points.

The laser irradiance plays a much more important role when fluorophores are attached in pairs as shown in Fig. 9. In this case, the acceptor attached to the same molecule as the donor is usually the closest target for energy transfer. Thus, if it is not available when a donor becomes excited, then energy transfer is much less likely to occur. Ideally FRET measurements should be made with the lowest laser irradiance that produces a decent signal.

Energy transfer in pentameric structures

As a more complex example of the use of the Monte Carlo calculation scheme, we examine the case where fluorophores are attached to a pentameric protein. This situation provides a useful model of ligand-gated ion channels, in which the fluorophores compete to bind to an identical site within each subunit of the protein.

Energy transfer within a single pentamer

Energy transfer within a pentamer of fluorophores can be calculated analytically, if the rate of energy transfer is less than the rate of incoming photons that are absorbed (i.e., if irradiance ≈ 0), or numerically in the more general case. The derivation of the analytic solution is in Appendix A.

The efficiencies of energy transfer within an isolated pentameric structure are shown in Fig. 10. It can be seen that the numerical results from the Monte Carlo calculation scheme (*data points*) agree well with the analytic solution (*lines*), which provides a good test of the Monte Carlo method. It is worth noting that the FRET efficiency does not approach *1* as the radius of the pentamer goes to *0*, because there is always a possibility that all five sites will be occupied by either donors or acceptors, in which case FRET cannot take place.

In Fig. 10, we also examine how the efficiency of energy transfer alters as we change the ratio of donors to acceptors. Interestingly, the greatest transfer efficiency arises when there are equal probabilities of any site being occupied by a donor or acceptor. Unlike the cases described earlier, it is not advantageous to have more acceptor than donor molecules to increase FRET. In such cases, the chance of having all five sites in the pentamer occupied by acceptors increases. Indeed, the chance of having either five donors and no acceptors, or five acceptors and no donors (and thus no FRET), is 0.06, 0.24, and 0.59 for the cases of 50%, 25%, and 10% donors, respectively. This probability directly determines the maximum FRET efficiency that will be seen for such pentameric structures.

Pentamers distributed in two dimensions

So far we have considered only a single pentamer, isolated such that it does not interact with any other. In reality, the pentameric proteins are likely to be suspended in a solution or lipid membrane, and unless the density of protein is extremely low, there will always be a chance that transfer will take place between donors in one pentamer and acceptors in another. This situation can again be dealt with using the Monte Carlo scheme. Here, we concentrate on the case of the pentamers being distributed in a plane, as would be the case if we were examining pentameric ion channels confined within a lipid membrane.

Fig. 11 shows a number of pentamers of radius 30 Å distributed randomly in a plane at a density of 2×10^{-5} pentamers/Å^2 as described in Methods, above. It is clear that some pentamers lie close to one another and that FRET between pentamers (*ext*) will be just as likely as FRET within the pentamers (*int*) in some cases.

The FRET efficiency is again calculated using the Monte Carlo program in a number of situations. It is important to

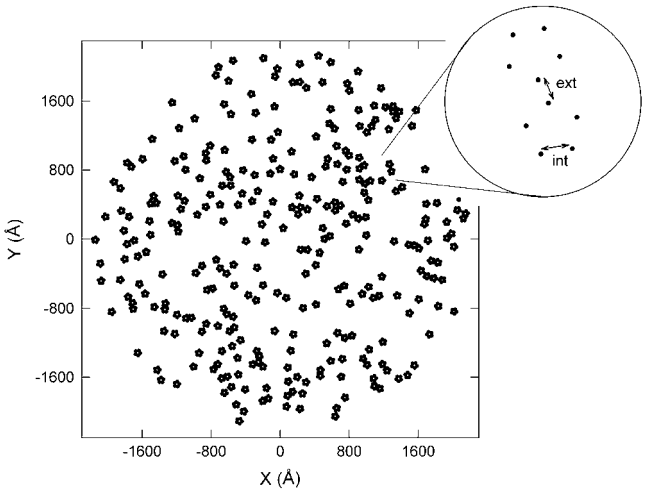

FIGURE 11 An example distribution of pentamerically linked fluorophores confined to a plane as used for the Monte Carlo calculations. The distribution shown contains 300 radius 30 Å pentamers at a density of 2×10^{-5} pentamers/Å^2. FRET can arise between fluorophores in the same pentamer (*int*) or with fluorophores in neighboring pentamers (*ext*), as shown in the zoom-in at the top right.

note that, as discussed in Methods, the calculation is made for thousands of configurations such as shown in Fig. 11, for each set of input parameters, to make sure that reliable average values are obtained.

In Fig. 12, we relate the FRET efficiency to the radius of the pentamer for various choices of R_0 at a pentamer density of 2.0×10^{-5} pentamers/Å^2. In each case, the efficiency is critically dependent on the radius of the pentamer, and so, provided an appropriate pair of fluorophores is chosen to match the pentamer radius, the dimensions of the pentamer can be accurately determined from a measurement of FRET from an ensemble of molecules. It is clear that the transfer efficiency does not drop to zero as the pentamer radius gets large. This is a result of transfer between fluorophores in different pentamers which becomes more likely at large radius.

Energy transfer between pentamers is again more likely to arise as their density in the plane increases, as shown in Fig. 13 for three different pentamer radii. In Fig. 13 *A* we plot the density in terms of pentamers per square Å, whereas in Fig. 13 *B* we show the same data using a more commonly used experimental measure of pentamer density, the lipid/pentamer (or protein) ratio (by number). In this second case, we calculate the ratio by assuming each lipid molecule in the plane occupies a surface area of 66 Å^2, based roughly on the density in a phosphatidylcholine lipid monolayer calculated from a molecular dynamics simulation. Dividing this by two, assuming the lipid forms a bilayer and inverting, gives a lipid density of 0.03 lipid molecules per Å^2. It can be seen that the pentamer density is again important; however, pentamers of different radii can be clearly distinguished even if the pentamer density is not accurately known.

CONCLUDING REMARKS

The Monte Carlo calculation scheme presented here provides a simple and flexible way to calculate energy transfer

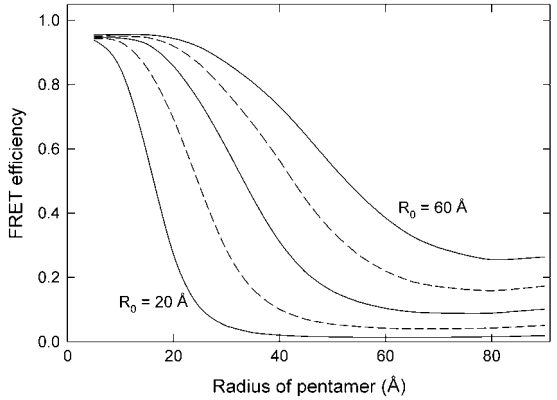

FIGURE 12 Efficiency of energy transfer for many fluorophores linked in pentamers and distributed randomly in a plane. The efficiency is plotted against the radius of the pentamers for a number of characteristic distances ($R_0 = 20$, 30, 40, 50, and 60 Å). The density of pentamers was set to 2.0×10^{-5} pentamers/Å^2 and the irradiance is assumed to be small.

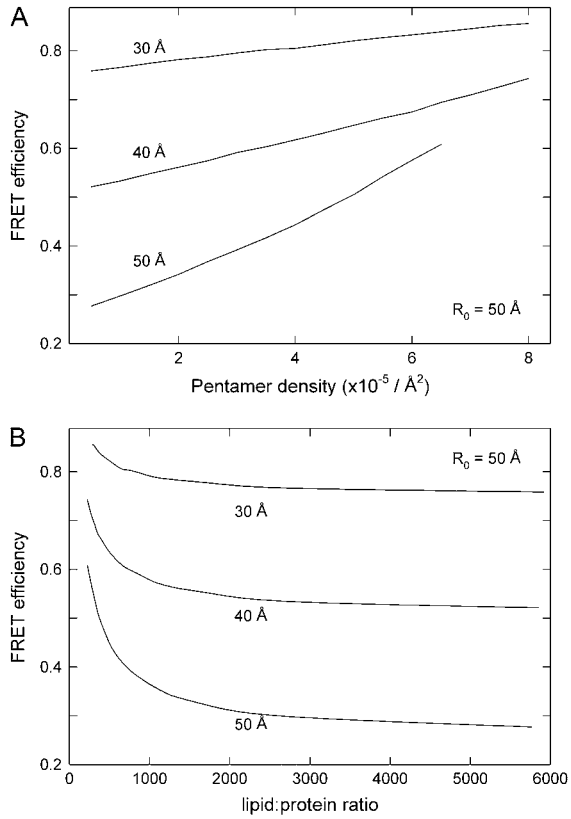

FIGURE 13 The influence of pentamer density on transfer efficiency for fluorophores linked in pentamers distributed in a plane. The efficiency is plotted against the pentamer density represented either by a number density (*A*) or the lipid/protein ratio (by number) (*B*) for pentamers of three different radii (30, 40, and 50 Å) with $R_0 = 50$ Å.

efficiencies for complex distributions of fluorophores. We have used it to predict the efficiency for fluorophores randomly distributed in two and three dimensions, linked in donor-acceptor pairs with excluded volumes, and linked in pentamers. We found good agreement between the predictions of the model and experimental measurements for the case of fluorophores distributed in three dimensions. Furthermore, when donor acceptor pairs are attached to the same host molecule, and when the hosts are at low concentration, the model reproduces Förster's well-known $1/r^6$ relationship that has been well verified (34). Although it is beyond the scope of this article to test every situation described in an experimental manner, these two results suggest that the simulation scheme accurately describes FRET taking place between both fluorophores on the same host as well as those on different host molecules.

We find that the efficiency of energy transfer is strongly dependent upon the characteristic distance of energy transfer, R_0, and the density of fluorophores. If we assume that already excited fluorophores cannot participate in energy transfer until they de-excite, then the incident flux of photons plays a role in determining the energy transfer efficiency. Using low power lasers this may not be a significant effect, however; using high power lasers without transmission filters could significantly reduce the transfer efficiency as well as bleaching the fluorophores. The ratio of donors to acceptors is also important in determining the rate of energy transfer. In most situations having many acceptors for every donor leads to an increase in energy transfer efficiency. However, in some situations, such as the linked pentamers of fluorophores, the average efficiency is greatest when the number of donors equals the number of acceptors.

The scheme presented here can easily be extended to deal with any arrangement of fluorophores, taking into account regions of any shape where fluorophores cannot reside, or links between them. Throughout his study, we have assumed that the rate of diffusional motion is slow compared to the rate of energy transfer, such that the donor-acceptor distance does not change during transfer. Given that we sample a large number of random configurations, we are likely to be capturing the variety of possible distances and so diffusion is unlikely to alter the results. It would be possible, though, to include diffusional motion during the calculation if this were deemed to be important. Also, it would be possible to allow for photobleaching of individual fluorophores (30) or for the characteristic distance of energy transfer, R_0, to change with the distance from the donor or be different for different donor-acceptor pairs. We do not assume any particular value of the orientation factor κ^2, but rather incorporate it into the input parameter R_0. If κ^2 were known, this could be used to specify the value of R_0. Alternatively, if the distances between donor and acceptor fluorophores were already known, this model could be used to work backward to determine the relative orientation of the fluorophores. We have also assumed that the host molecules are randomly distributed in two or three dimensions. If some degree of clustering of the host's molecules was known to occur, this would have to be taken into account when creating fluorophore configurations (Step 1.2). Additionally, the model could be extended to cases where the donor and acceptor fluorophores are attached to separate hosts.

This technique provides a powerful tool for examining resonance energy transfer among ensembles of particles as well as for single molecules to which many fluorophores are attached. Being able to relate the transfer efficiency to the geometry of fluorophores in this way means that FRET can be used to gain quantitative information in a range of new experimental systems. In an accompanying article, we demonstrate the use of this technique for determining the conformational changes involved in gating the mechanosensitive channel MscL (35).

APPENDIX A: ANALYTIC EXPRESSION FOR THE TRANSFER EFFICIENCY IN A PENTAMERIC STRUCTURE

In a pentamer, there are two possible distances between fluorophores: r_a, the side length of a pentagon, and r_b the diagonal, as shown in Fig. 14. It can be calculated that

$$r_b = \frac{1+\sqrt{5}}{2} r_a \equiv \gamma r_a, \tag{15}$$

where γ is the golden ratio. Using Eq. 3, the efficiency of energy transfer from a donor at these two distances is given by

$$E_a = \frac{1}{1+\left(\frac{r_a}{R_0}\right)^6} \quad \text{and} \quad E_b = \frac{1}{1+\left(\frac{r_b}{R_0}\right)^6}. \tag{16}$$

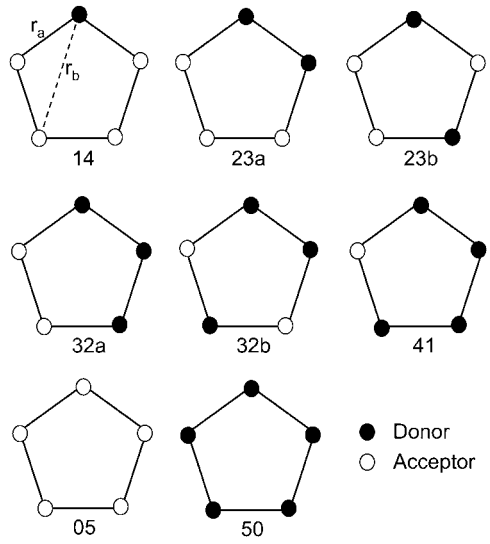

FIGURE 14 Possible distributions of donors and acceptors on a molecule with five binding sites. Each case is labeled by the number of donors followed by the number of acceptors. Where there are further possible configurations, this is denoted with the character *a* or *b*. The possible distances between fluorophores, r_a and r_b are noted.

We are interested in calculating the average transfer efficiency in such pentamers, taking into account all possible configurations of donors and acceptors. If the probability of any site being occupied by a donor or acceptor molecule is given by P_d and P_a, and we assume that all sites are occupied, then

$$P_d + P_a = 1. \tag{17}$$

The possible distinct pentamer configurations are shown in Fig. 14. In Table 3, we list these configurations and note the efficiency of energy transfer for each and probability of that configuration arising.

The individual efficiencies in the table can be calculated from the rates of energy transfer. For example, for the case of one donor and two acceptors (this case does not occur in the pentamer just discussed), the average rate of energy transfer is given by

$$\eta_{da}^{12} = \eta_{d,a1} + \eta_{d,a2} = \frac{R_0^6}{\tau_D}\left(\frac{1}{r_1^6} + \frac{1}{r_2^6}\right), \tag{18}$$

where r_1 and r_2 are the two distances between the donor and the acceptor, and the η-values are the rates of energy transfer. From Eq. 18, we get

$$E = \frac{\eta_{da}}{\eta_d + \eta_{da}} = \frac{R_0^6\left(\frac{1}{r_1^6} + \frac{1}{r_2^6}\right)}{1 + R_0^6\left(\frac{1}{r_1^6} + \frac{1}{r_2^6}\right)}, \tag{19}$$

where the rate of decay of the isolated donor is $\eta_d = \tau_D^{-1}$. Similarly, for two donors and one acceptor, the rate of transfer is given by the average of the rate of transfer from each donor to the acceptor,

$$\eta_{da}^{21} = \frac{1}{2}(\eta_{d1,a} + \eta_{d2,a}). \tag{20}$$

The factor ½ arises because any incoming photon is absorbed by, at most, one donor; hence the rate of transfer is the average of the rates over all the donors. Equivalently, the transfer efficiency can be expressed as the average of the transfer efficiency originating from each donor,

$$E_1 = \frac{R_0^6\left(\frac{1}{r_1^6}\right)}{1 + R_0^6\left(\frac{1}{r_1^6}\right)} \text{ and } E_2 = \frac{R_0^6\left(\frac{1}{r_2^6}\right)}{1 + R_0^6\left(\frac{1}{r_2^6}\right)}, \tag{21}$$

to yield

$$E = \frac{1}{2}(E_1 + E_2) = \frac{1}{2}\left(\frac{R_0^6\left(\frac{1}{r_1^6}\right)}{1 + R_0^6\left(\frac{1}{r_1^6}\right)} + \frac{R_0^6\left(\frac{1}{r_2^6}\right)}{1 + R_0^6\left(\frac{1}{r_2^6}\right)}\right). \tag{22}$$

In general for n_d donors and n_a acceptors,

$$E = \sum_{i=1}^{n_d}\left[\frac{R_0^6\sum_{j=1}^{n_a}\frac{1}{r_{ij}^6}}{1 + R_0^6\sum_{j=1}^{n_a}\frac{1}{r_{ij}^6}}\right]\frac{1}{n_d}, \tag{23}$$

where r_{ij} is the distance from the i^{th} donor to the j^{th} acceptor. By referring to Fig. 14 and noting that the only distinct distances between donor and acceptor are

$$r_{ij} = r_1 \quad \text{or} \quad r_{ij} = \gamma r_1, \tag{24}$$

we get the following expressions for the efficiencies in the table:

$$E_{14} = \frac{R_0^6\left(\frac{2}{r_1^6} + \frac{2}{\gamma^6 r_1^6}\right)}{1 + R_0^6\left(\frac{2}{r_1^6} + \frac{2}{\gamma^6 r_1^6}\right)}, \tag{25}$$

$$E_{23a} = \frac{R_0^6\left(\frac{1}{r_1^6} + \frac{2}{\gamma^6 r_1^6}\right)}{1 + R_0^6\left(\frac{1}{r_1^6} + \frac{2}{\gamma^6 r_1^6}\right)}, \tag{26}$$

$$E_{23b} = \frac{R_0^6\left(\frac{2}{r_1^6} + \frac{1}{\gamma^6 r_1^6}\right)}{1 + R_0^6\left(\frac{2}{r_1^6} + \frac{1}{\gamma^6 r_1^6}\right)}, \tag{27}$$

$$E_{32a} = \frac{2}{3}\left[\frac{R_0^6\left(\frac{1}{r_1^6} + \frac{1}{\gamma^6 r_1^6}\right)}{1 + R_0^6\left(\frac{1}{r_1^6} + \frac{1}{\gamma^6 r_1^6}\right)} + \frac{R_0^6\left(\frac{1}{\gamma^6 r_1^6}\right)}{1 + R_0^6\left(\frac{2}{\gamma^6 r_1^6}\right)}\right], \tag{28}$$

$$E_{32b} = \frac{2}{3}\left[\frac{R_0^6\left(\frac{1}{r_1^6} + \frac{1}{\gamma^6 r_1^6}\right)}{1 + R_0^6\left(\frac{1}{r_1^6} + \frac{1}{\gamma^6 r_1^6}\right)} + \frac{R_0^6\left(\frac{1}{r_1^6}\right)}{1 + R_0^6\left(\frac{2}{r_1^6}\right)}\right], \tag{29}$$

$$E_{41} = \frac{1}{2}\left[\frac{R_0^6\left(\frac{1}{r_1^6}\right)}{1 + R_0^6\left(\frac{1}{r_1^6}\right)} + \frac{R_0^6\left(\frac{1}{\gamma^6 r_1^6}\right)}{1 + R_0^6\left(\frac{1}{\gamma^6 r_1^6}\right)}\right]. \tag{30}$$

With the above equations, the total efficiency of FRET will be the sum of the efficiency for a particular configuration, times the probability that the configuration will occur. Thus, the average efficiency for many such isolated pentamers will be

$$E(r_1, P_d) = P_{41}E_{41} + P_{32}(E_{32a} + E_{32b}) + P_{23}(E_{23a} + E_{23b}) + P_{14}E_{14}, \tag{31}$$

TABLE 3 Possible configurations of pentamers of fluorophores and their associated FRET efficiencies

No. of donors, n_d	No. of acceptors, n_a	Additional case label	Efficiency E	No. of distinct arrangements, n	Probability per case
5	0		0	1	P_d^5
4	1		E_{41}	5	$P_d^4P_a$
3	2	a	E_{32a}	5	$P_d^3P_a^2$
3	2	b	E_{32b}	5	$P_d^3P_a^2$
2	3	a	E_{23a}	5	$P_d^2P_a^3$
2	3	b	E_{23b}	5	$P_d^2P_a^3$
1	4		E_{14}	5	$P_dP_a^4$
0	5		0	1	P_a^5

where

$$P_{41} = 5\,P_{\mathrm{d}}^{4}\,P_{\mathrm{a}}, \tag{32}$$

$$P_{32} = 5\,P_{\mathrm{d}}^{3}\,P_{\mathrm{a}}^{2}, \tag{33}$$

$$P_{23} = 5\,P_{\mathrm{d}}^{2}\,P_{\mathrm{a}}^{3}, \tag{34}$$

TABLE 4 List of input parameters to the ExiFRET program, their allowed values and meanings

Input	Allowed values	Meaning
system_dimension	2,3	The number of dimension in which fluorophores are to be distributed.
nmer_size	≥1	Number of fluorophores per *n*-mer, i.e., on each host molecule.
da_pairs	.true. or .false.	If nmer_size = 2, do you want every pair to have one donor and one acceptor? Ignored for other *n*-mer sizes.
n_densities	≥1	Number of concentrations of *n*-mers for which to calculate transfer efficiency (E).
density_min	>0.0	Minimum *n*-mer concentration.
density_max	≥density_min	Maximum *n*-mer concentration.
n_radius	≥1	Number of *n*-mer radii for which to calculate *E*.
radius_min	>0.0	Minimum *n*-mer radii.
radius_max	≥radius_min	Maximum *n*-mer radii.
avoid_overlap	.true. or .false.	Include excluded regions?
planar_nmers	.true. or .false.	If system_dimension = 3, do you want fluorophores on each *n*-mer to be distributed in a plane (.true.) or on a sphere (.false.)?
r0	>0.0	The characteristic or Förster distance of donor acceptor pairs in Å.
n_particles	≥1	Number of *n*-mers in each configuration.
n_configurations	≥1	Number of configurations of *n*-mers to average before outputting FRET efficiency.
p_donor	[0,1]	Probability of any given fluorophore being a donor.
n_excitons	≥1	Number of excitons to use in each transfer efficiency calculation.
buffer_size	∈ R	Fluorophores within buffer_size $\times R_0$ of the edge of the system are not included in efficiency calculation.
irradiance	>0.0	Irradiance of the illuminating laser in units of Watts per square μm.
wavelength	>0.0	Wavelength of the illuminating laser in nanometers.
extinction_coefficient	>0.0	Extinction coefficient of the donor molecules in $\mathrm{cm}^{-1}\,\mathrm{M}^{-1}$.
donor_lifetime	>0.0	The lifetime of donor excitation in the absence of acceptors in nanoseconds (experimental data usually available).
acceptor_lifetime	>0.0	The lifetime of acceptor excitation in ns (experimental data usually available).

$$P_{14} = 5\,P_{\mathrm{d}}P_{\mathrm{a}}^{4}. \tag{35}$$

Similar expressions can be calculated assuming that some sites remain unoccupied, or if pentamers of two different sizes (such as closed- and open-state ion channels) are present in the sample.

APPENDIX B: COMPUTER PROGRAM EXIFRET

As noted in the text, a program for conducting the Monte Carlo calculations described in this article entitled ''ExiFRET'' (short for ''exciton FRET'') has been developed. The code is available to interested readers upon request. A description of the program inputs is included in Table 4.

The program outputs the efficiency of energy transfer values for the situations specified by the input file. The exact format of the output differs depending on the properties of the system considered, but includes the *n*-mer radius, *n*-mer concentration, system size, and FRET efficiency value. Coordinates of example fluorophore configurations are also output.

The authors thank Professor Boris Martinac for his helpful discussions.

This work was supported by funding from the Australian Research Council, the National Health and Medical Research Council, and The University of Western Australia. The authors also acknowledge support of the Biomedical Imaging and Analysis Facility by LotteryWest.

REFERENCES

1. Förster, T. 1959. Transfer mechanisms of electronic excitation. *Discuss. Faraday Soc.* 27:7–17.
2. Van Der Meer, B. W., G. Coker, and S. Y. S. Chen. 1994. Resonance Energy Transfer: Theory and Data. VCH, New York.
3. Clegg, R. M. 1996. Fluorescence resonance energy transfer (FRET). *In* Fluorescence Imaging Spectroscopy and Microscopy. X.F. Wang and B. Herman, editors. Wiley, New York. 179–252.
4. Jares-Erijman, E. A., and T. M. Jovin. 2003. FRET imaging. *Nat. Biotechnol.* 21:1387–1395.
5. Haas, E., M. Wilchek, E. Katchalski-Katzir, and I. Z. Steinberg. 1975. Distribution of end-to-end distances of oligopeptides in solution as estimated by energy transfer. *Proc. Natl. Acad. Sci. USA.* 72:1807–1811.
6. Lakowicz, J. R., I. Gryczynski, W. Wiczk, G. Laczko, F. C. Prendergast, and M. L. Johnson. 1990. Conformational distributions of melittin in water/methanol mixtures from frequency-domain measurements of nonradiative energy transfer. *Biophys. Chem.* 36: 99–115.
7. Chapman, E. R., K. Alexander, T. Vorherr, E. Carafoil, and D. R. Storm. 1992. Fluorescence energy transfer analysis of calmodulin-peptide complexes. *Biochemistry.* 31:12819–12825.
8. Heyduk, T. 2002. Measuring protein conformational changes by FRET/LRET. *Curr. Opin. Biotechnol.* 13:292–296.
9. Hink, M. A., T. Bisselin, and A. J. Visser. 2002. Imaging protein-protein interactions in living cells. *Plant Mol. Biol.* 50:871–883.
10. Parsons, M., B. Vojnovic, and S. Ameer-Beg. 2004. Imaging protein-protein interactions in cell motility using fluorescence resonance energy transfer (FRET). *Biochem. Soc. Trans.* 32:431–433.
11. Bunt, G., and F. S. Wouters. 2004. Visualization of molecular activities inside living cells with fluorescent labels. *Int. Rev. Cytol.* 237:205–277.
12. Lakowicz, J. R. 1999. Principles of Fluorescence Spectroscopy, 2nd Ed. Kluwer, New York.
13. Selvin, P. R. 2000. The renaissance of fluorescence resonance energy transfer. *Nat. Struct. Biol.* 7:730–734.
14. Berney, C., and G. Danuser. 2003. FRET or no FRET: a quantitative comparison. *Biophys. J.* 84:3992–4101.

15. Ha, T. 2001. Single-molecule fluorescence resonance energy transfer. *Methods*. 25:78–86.

16. Li, H., L. Ying, X. Ren, S. Balasubramanian, and D. Klenerman. 2004. Fluorescence studies of single biomolecules. *Biochem. Soc. Trans*. 32: 753–756.

17. Ha, T. 2001. Single-molecule fluorescence methods for the study of nucleic acids. *Curr. Opin. Struct. Biol*. 11:287–292.

18. Yildiz, A., M. Tomishige, R. D. Vale, and P. R. Selvin. 2004. Kinesin walks hand-over-hand. *Science*. 303:676–678.

19. Johnson, C. K., K. D. Osborn, M. W. Allen, and B. D. Slaughter. 2005. Single-molecule fluorescence spectroscopy: new probes of protein function and dynamics. *Physiology*. 20:10–14.

20. Deniz, A. A., M. Dahan, J. R. Grunwell, A. E. Faulhaber, T. Ha, D. S. Chemla, S. Weiss, and P. G. Schultz. 1999. Single-pair fluorescence resonance energy transfer on freely diffusing molecules: observation of Förster distance dependence and subpopulations. *Proc. Natl. Acad. Sci. USA*. 96:3670–3675.

21. Dietrich, A., V. Buschmann, C. Muller, and M. Sauer. 2002. Fluorescence resonance energy transfer (FRET) and competing processes in donor-acceptor substituted DNA strands: a comparative study of ensemble and single-molecule data. *J. Biotechnol*. 82:211–231.

22. Tweet, A. O., W. D. Bellamy, and G. L. Gains. 1964. Fluorescence quenching and energy transfer in monomolecular films containing chlorophyll. *J. Chem. Phys*. 41:2068–2077.

23. Fung, B. K. K., and L. Stryer. 1978. Surface density determination in membranes by fluorescence energy transfer. *Biochemistry*. 17:5241–5248.

24. Koppel, D. E., P. J. Fleming, and P. Strittmatter. 1979. Intramembrane positions of membrane bound-bound chromophores determined by excitation energy transfer. *Biochemistry*. 24:5450–5457.

25. Wolber, P. K., and B. S. Hudson. 1979. An analytic solution to the Förster energy transfer problem in two dimensions. *Biophys. J*. 28:197–210.

26. Dewey, T. G., and G. G. Hammes. 1980. Calculation of fluorescence resonance energy transfer on surfaces. *Biophys. J*. 32:1023–1036.

27. Snyder, B., and E. Freire. 1982. Fluorescence energy transfer in two dimensions. a numeric solution for random and nonrandom distributions. *Biophys. J*. 40:137–148.

28. Zimet, D. B., B. J. Thevenin, A. S. Verkman, S. B. Shohet, and J. R. Abney. 1995. Calculation of resonance energy transfer in crowded biological membranes. *Biophys. J*. 68:1592–1603.

29. Demidov, A. A. 1999. Use of Monte Carlo method in the problem of energy migration in molecular complexes. *In* Resonance Energy Transfer. D.L. Andrews and A.A. Demidov, editors. Wiley, New York. 435–465.

30. Frederix, P., E. L. de Beer, W. Hamelink, and H. C. Gerritsen. 2002. Dynamic Monte Carlo simulations to model FRET and photobleaching in systems with multiple donor-acceptor interactions. *J. Phys. Chem. B*. 106:6793–6801.

31. Hille, B. 2001. Ionic Channels of Excitable Membranes, 3rd Ed. Sinauer Associates, Sunderland, MA.

32. Förster, T. 1948. Intermolecular energy migration and fluorescence. *Ann. Phys*. 2:55–75.

33. Pawley, J. B. 1995. Handbook of Biological Confocal Microscopy, 2nd Ed. Plenum Press, New York.

34. Stryer, L. 1978. Fluorescence energy transfer as a spectroscopic ruler. *Annu. Rev. Biochem*. 47:819–846.

35. Corry, B., P. Rigby, Z. W. Liu, and B. Martinac. 2005. Conformational changes involved in MscL channel gating measured using FRET spectroscopy. *Biophys. J*. 89:L49–L51.